International Journal of Technology

http://ijtech.eng.ui.ac.id

Research Article

Influence of the Strong Green-Emission Phosphor $SrLaAlO_4$: Yb/Er@SiO_2 on the Illumination of Solid-State White Light-emitting Didoes

Phan Xuan Le[1], Nguyen Thi Phuong Loan[2*]

[1]Faculty of Electrical Engineering Technology, Industrial University of Ho Chi Minh City, Ho Chi Minh City, 70000, Vietnam

[2]Faculty of Fundamental 2, Posts and Telecommunications Institute of Technology, Ho Chi Minh City, 70000, Vietnam

*Corresponding author: ntploan@ptithcm.edu.vn; Tel.: +84-937994664

Abstract: The Yb^{3+}/Er^{3+} co-doped $SrLaAlO_4$(SLA: Yb^{3+}/Er^{3+}) phosphor is a potential upconversion luminescent material with strong green emission for high-power white light-emitting diodes (LEDs). This work used the SLA: Yb^{3+}/Er^{3+} phosphor for the white LED by blending it with yellow phosphor and SiO_2 particles, which is called the SLA: Yb/Er@SiO_2 mixture. The SLA: Yb^{3+}/Er^{3+} phosphor was created with a steady Er^{3+} ion concentration of 2 mol%, while that of the Yb^{3+} was adjusted in 1-7 mol%. Under the infrared laser excitation (980 nm), the collected data on luminescence measurement shows that the SLA: Yb^{3+}/Er^{3+} exhibited both upconversion green and red-color emissions in its luminescence band. Moreover, with 4 mol% of Yb^{3+}, the highest green-emission intensity was observed. A fabricated white LED comprising SLA: Yb/Er@SiO_2 compound placed on the blue LED chip was examined with different SiO_2 amounts. The obtained data showed an increase in the green luminescence power and lumen output of the white LED with increasing SiO_2 concentration. The presence of SLA: Yb/Er@SiO_2 helped reduce the color deviation for enhanced color uniformity. Thus, this green-emission SLA: Yb/Er@SiO_2 compound can be a competitive material for the development of solid-state lighting.

Keywords: Color uniformity; Lumen output; $SrLaAlO_4$; Upconversion phosphor; White LED; Yb/Er@SiO_2

1. Introduction

Recently, the development of luminescence phosphors for light-emitting diodes (LEDs) has been a topic of research and has played an important role in enhancing the quality of solid-state illumination (Le et al., 2025; Tung et al., 2024c; Kumari et al., 2022). Solid-state light-emitting diode (LED) lighting has been applied in many fields, including displaying, traffic and transportation lighting, commercial and industrial lighting, and advanced sensing and bioimaging (Ma et al., 2024). The conventional light-emitting diode (LED) model comprises a blue chip and a downconversion $Y_3Al_5O_{12}:Ce^{3+}$ (YAG:Ce^{3+}) yellow phosphor (Tung et al., 2024b; Chen et al., 2020). The yellow phosphor was placed on the blue chip to convert the blue emission to yellow emission and induce the combination of blue and yellow light for white light generation (Cong and Anh, 2025; Nguyen and Nguyen, 2025). This combination was recognized for its high luminescence, but its well-known downside is low color rendition owing to the weak green and orange-red emission color in the created white light wavelength of the package (Hanh et al., 2025; Le et al., 2025).

The $MAAlO_4$ (M = Ca, Sr; A = metals, yttrium, rare-earth ions) composition has drawn a lot of attention owing to its tetragonal symmetry (Loan and Anh, 2021; Luo et al., 2020; Thi et al., 2020), I4/mmm space group, and unit-cell size, which are suitable as host materials for

https://doi.org/10.14716/ijtech.v17i3.6327
Received January 2023; Revised June 2023; Accepted July 2023

luminescent phosphors used in LED lighting and imaging. Some of them, such as $CaNdAlO_4$ and $SrLaAlO_4$, were used as hosts for doping Yb^{3+} and Ho^{3+} to generate yellow to red emissions via the upconversion mechanism. Nevertheless, compared with downconversion materials, upconversion materials produce less intense luminescence (Trang et al., 2025; Chou et al., 2022). Additionally, for the upconversion phosphor to emit light in visible wavelengths, the excitation source should be in the region from 920 to 980 nm, which are the emission wavelengths of lasers. Meanwhile, blue and ultraviolet (UV) sources can excite the phosphor to produce visible-wavelength light, which is simpler than the upconversion phosphors, for the downconversion type (Le et al., 2022; Le et al., 2021; That et al., 2020b). Thus, combining the laser and upconversion luminescence materials to produce LED could be more complex and difficult for manufacturers (Le et al., 2021; Thi et al., 2021).

The $SrLaAlO_4$ host reportedly possesses outstanding features, including consistent dielectric, thermodynamic, optical, and superconducting properties. It was integrated with Tb^{3+}, Yb^{3+}, or Er^{3+} to achieve green or red emission by the upconversion route. However, the luminescence from these compositions was still weaker than that obtained from the downconversion material with the same host (My et al., 2023; Chen et al., 2020). Thus, to improve the luminescence efficiency of the white LED using $SrLaAlO_4$–host upconversion phosphor, this work investigates the combination of Yb^{3+}/Er^{3+} co-doped $SrLaAlO_4$ (SLA: Yb^{3+}/Er^{3+}) phosphor and SiO_2 to provide better green emission for the solid-state white LED. The phosphor was prepared with a fixed concentration of Er^{3+} (2 mol%) and varying dosage of Yb^{3+} (1-7 mol%). The Yb^{3+} plays a role as a sensitizer for energy transfer to Er^{3+} ions, improving green emission spectra (Tung et al., 2024a; Loan et al., 2022; Thuy et al., 2022). Subsequently, the suggested phosphor compound (SLA: Yb/Er@SiO_2) was coupled with a blue-pumped LED chip and YAG: Ce^{3+} phosphor to produce an LED package. The concentration of SLA: Yb^{3+}/Er^{3+} is constant while that of the SiO_2 varies to regulate the scattering property of the compound. The results showed that increasing SiO_2 amount can help increase the luminous intensity and light transmitting power of the whole package, suggesting the potential of SLA: Yb/Er@SiO_2 phosphor compound in solid-state LED lighting.

2. Methods

2.1 Synthesis of SLA: Yb^{3+}/Er^{3+} phosphor

All raw ingredients of SLA: Yb^{3+}/Er^{3+} chemical composition were obtained from Sigma-Aldrich (St. Louis, MO, USA) and are shown in Table 1. Table 2 Detailed the synthesis process. In the preparation process of SLA: Yb^{3+}/Er^{3+} phosphor, the Er^{3+} ion dopant amount was steady at 2 mol%, as previous studies demonstrated that 2 mol% Er^{3+} was the optimal concentration to produce the strongest green emission Er^{3+}-doped compositions, including ZrO_2: Er^{3+} and Y_2O_3: Er^{3+},Yb^{3+}, and in $SrLaAlO_4$ geometry (Nguyen et al., 2025; Sun et al., 2024).The concentration of Yb^{3+} was adjusted in the range of 1-7 mol% and finally selected at 4 mol% because the highest emission strength of the sample was recorded at 4 mol% Yb^{3+} dopant (Nguyen and Nguyen, 2025; Zhan et al., 2024; Loan et al., 2022).

Table 1 Ingredients of SLA: Yb^{3+}/Er^{3+} chemical composition

Ingredients	Purity (%)
$Sr(NO_3)_2{\cdot}6H_2O$	≥99%
$La(NO_3)_3{\cdot}6H_2O$	≥99%
$Al(NO_3)_3{\cdot}9H_2O$	≥99%
$Er(NO_3)_3{\cdot}5H_2O$	≥99%
$Yb(NO_3)_3{\cdot}5H_2O$	≥99%
CH_4N_2O	≥99%

Table 2 SLA: Yb^{3+}/Er^{3+} synthesis procedure

Stage	Process
Mixing	
	• The listed nitrate materials were blended stoichiometrically with distilled water (25 ml).
	• Then, the mixture is stirred for 15 minutes to get all ingredients well blended.
	• The last step of the mixing stage is to add 15 ml of CH_4N_2O solution (aqueous) to the as-prepared mixture and stir the new mixture slowly (within 10 min).
Heating	
	• The first heating time for the obtained solution is carried out at 90°C to obtain the gel form.
	• The next heating time is operated at 650°C in a furnace for 15 min to obtain the white foam.
	• Before proceeding to the final heating time, the white foam obtained is ground into powders.
	• The annealing process for the powders lasts 6 hours at 1000°C in air with 10°C/min heating rate.
Doping Er^{3+} and Yb^{3+}	
	• The attained $SrLaAlO_4$ was doped with 2 mol% Er^{3+} and 1–7 mol% Yb^{3+}.

2.2 Characterization

The luminescence and structural characteristics of the obtained SLA: Yb^{3+}/Er^{3+} were examined using the instruments shown in Table 3. Note that the phosphor emission spectra measurements were carried out at room temperature.

Table 3 Instruments for SLA: Yb^{3+}/Er^{3+} characterization

Characteristics	Examining instruments
Particle morphology	Scan Mira3 LMU SEM (30 kV)
Energy-dispersive X-ray spectroscopy	Thermo Fisher Scientific EDS detector using a scanning electron microscope
X-ray diffraction (XRD)	Analytical Empyrean diffractometer operated with Cu-Kα radiation, 2θ of 20°–80°, 0.05° scan rate
Luminescence spectra	Ocean Optics USB6500 spectrophotometer with an infrared light-emitting diode (980 nm) excitation source
Phosphor lifetimes	Princeton Instruments Acton Pro SP350i fluorometer equipped with Hamamatsu R955 photomultiplier tube
Chromatic coordinates	Jenoptik complementary metal–oxide–semiconductor camera (excitation at 980 nm)
Luminance of the LED	Konica Minolta CS-2000 spectroradiometer

2.3 LED modeling

The LED model was built using the LED model was built using the prepared SLA: Yb^{3+}/Er^{3+} and YAG:Ce^{3+} phosphor integrated into the infrared LED chip packet (Cong et al., 2025; Trang and Anh, 2025; Lv et al., 2022).

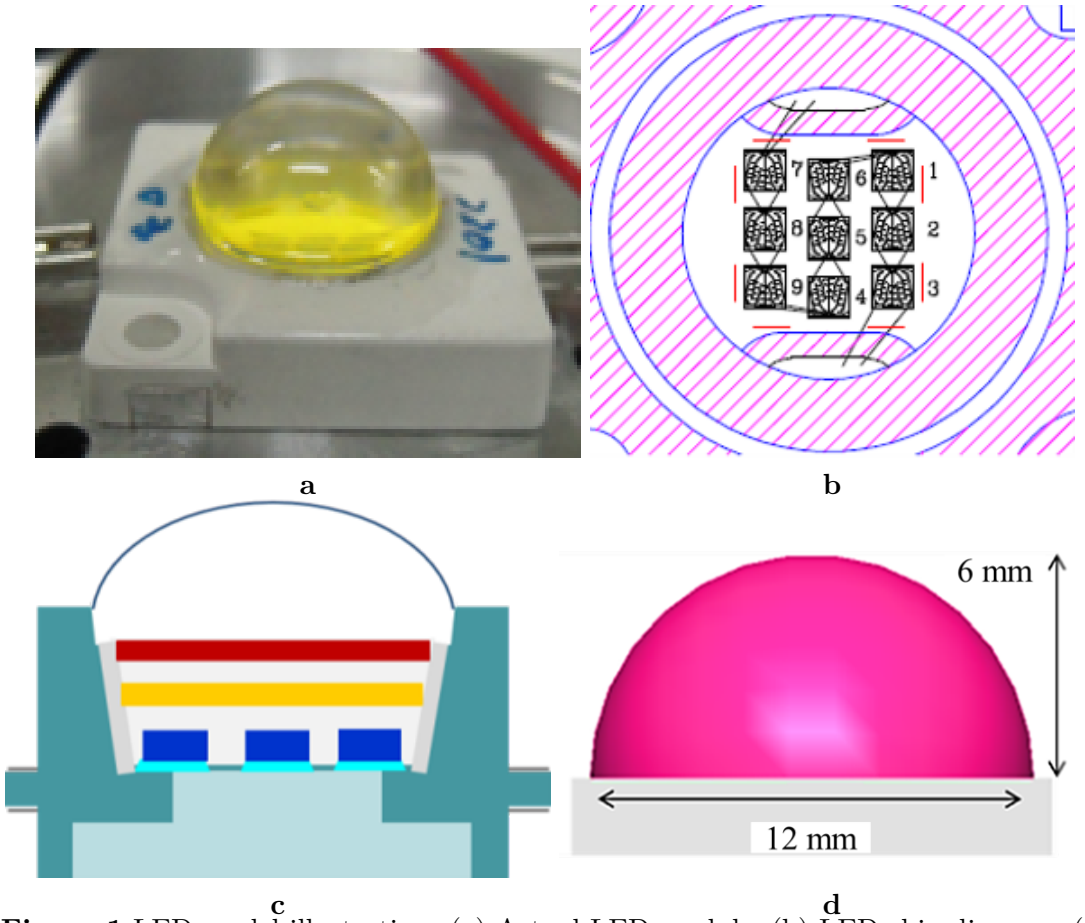

a b c d

Figure 1 LED model illustration: (a) Actual LED module; (b) LED chip diagram; (c) LED-model cross section; and (d) LightTools software-based LED simulation

Figure 1 shows the LED model used in this work. Figure 1a shows a real photo of the actual LED module. Figures 1b, 1c, and 1d show the chip packet diagram, the cross section of the built model in which the component arrangement is included, and the 3D simulation model obtained using the LightTools software, respectively (Anh et al., 2025a; Anh and Lee, 2024; Tung et al., 2024c). The chip has a wavelength of 465 nm, and the concentration of SiO_2 in the compound was varied in the range of 5-50 wt.%.

3. Results and Discussion

3.1 SLA: Yb^{3+}/Er^{3+} crystalline size and luminescence

The crystalline size (Cz) of the SLA: Yb^{3+}/Er^{3+} phosphor can be computed using the Scherrer equation in (1) (Deng et al., 2024):

$$C_z = \frac{k\lambda}{\beta \cos\theta} \tag{1}$$

where λ is equal to 1.5406 Å as the X-ray wavelength, k is equal to 0.94 (Gaudfrin et al., 2022; Lin et al., 2022), and θ denotes the Bragg angle. We observed that the Cz values decreased as the Yb^{3+} doping dosage increased (1-7 mol%), resulting in the enlargement in the surface

area, contributing to the improvement of the phosphor luminescence performance. Then, the phosphor luminescence lifetime was computed using the following expression (Cao et al., 2022):

$$I(t) = I(0) \times e^{-\frac{t}{\tau}} \quad (2)$$

where $I(t)$ and $I(0)$ are the luminescence intensities at time t and 0, respectively; and τ represents the lifetime parameter.

The phosphor exhibited notable emission centers in the green and red regions, in 531-553 nm and 655-675 nm, respectively. Furthermore, the emission in the green wavelength band is significantly stronger than that in the red region (Luo et al., 2020; That et al., 2020a; That et al., 2020b).The noticeable emission centers in the green and red wavelength bands can be attributed to the ion Er3+ transitions of $^2H_{11/2} + {}^4S_{3/2} \rightarrow {}^4I_{15/2}$ and $^4F_{9/2} \rightarrow {}^4I_{15/2}$, respectively. Moreover, when doping the Yb3+ ion together with the Er^{3+}, the Yb^{3+} acts as a sensitizer to the Er^{3+}, enabling red-emission and stimulating the green luminescence. When the concentration of Yb^{3+} dopant was 4 mol%, the phosphor emission strength was the highest; thus, we decided to use the sample SLA: 4%Yb^{3+}/2%Er^{3+} to fabricate the tested LED model (Wang et al., 2025; Liang et al., 2022).

3.2 SLA: Yb/Er@SiO2 effects on lighting performance

When integrating the SLA: Yb/Er@SiO_2 compound, in addition to the YAG:Ce^{3+} yellow phosphor, the scattering performance, the amount of YAG:Ce^{3+} dopant, and the correlated color temperature (CCT) were impacted, as shown in Figures 2 and 3, respectively.

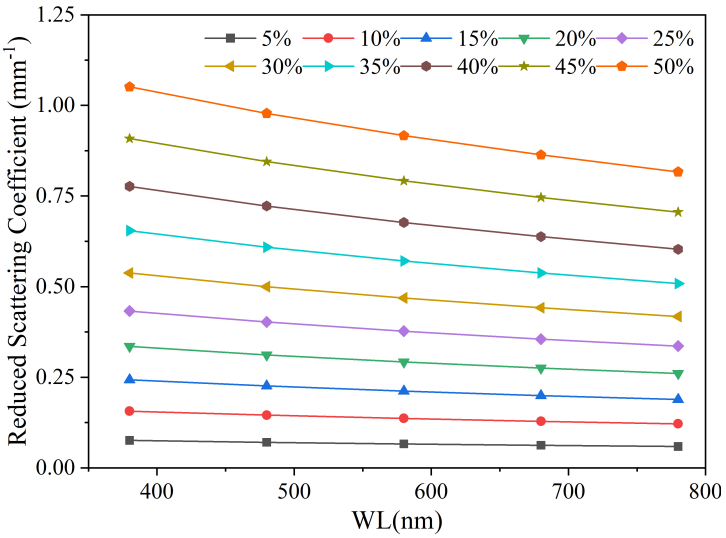

Figure 2 Reduced scattering coefficients of LED light with increasing SiO_2 concentration (5-50wt.%) in SLA: Yb/Er@SiO_2 compound. WL (nm) is the abbreviation for wavelength (nm)

In particular, the reduced scattering coefficients of the LED light in the presence of SLA: Yb/Er@SiO_2 (Figure 2) increased with the higher concentration of SiO_2 amounts in the compound, especially in the case of shorter light wavelengths. This indicates that less light was reflected and reabsorbed, leading to a higher amount of light rays getting out of the package for luminous improvement. The YAG:Ce^{3+} dosage and CCT of the LED light were also affected by the SiO_2 level, as shown by Figure 3. In Figure 3(a), it is easy to notice an inverse relationship between the YAG:Ce^{3+} and SiO_2 contents. The increase of SiO_2 contents in the SLA: Yb/Er@SiO_2 compound led to a decrease in the YAG:Ce^{3+} concentration, which stabilizes the color temperature and contributes to changing the scattering performance inside the LED model.

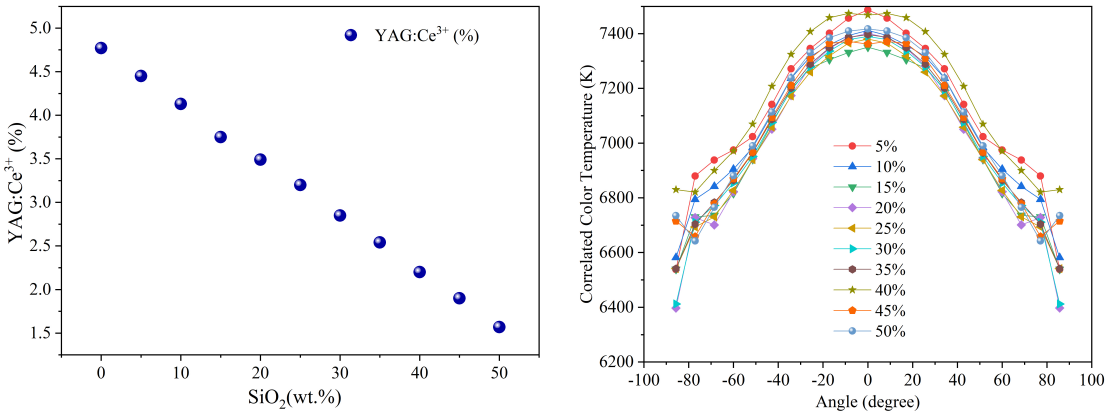

a b

Figure 3 The correlation of SiO_2 level (5-50wt.%) in SLA: Yb/Er@SiO_2 with (a) YAG:Ce^{3+} dosage and (b) CCT of LED light

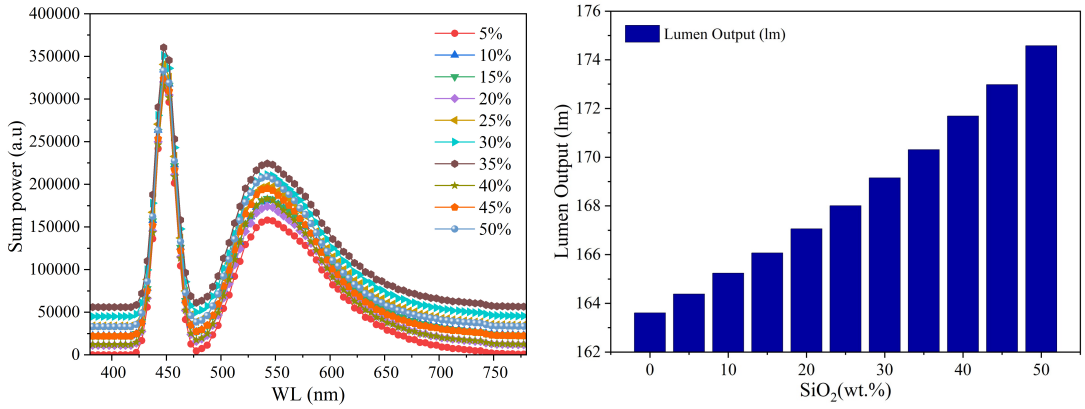

a b

Figure 4 The correlation of SiO_2 level (5-50wt.%) in SLA: Yb/Er@SiO_2 with (a) Transmission power and (b) Lumen output of LED light

Figure 3(b) presents the CCT values of the as-prepared LED as a function of increasing SiO_2 concentration. Initially, the increase in SiO2 amount caused the CCT values to slightly rise (with 5-20wt.% dopant). Then, as the SiO_2 concentration increased to 50wt.%, the CCT values decreased by a small amount. Specifically, in the viewing angle from -90∘ to 90∘, the CCT range between the highest and lowest values is approximately 875 K when the SLA: Yb/Er@SiO_2 compound is not integrated. As the SLA: Yb/Er@SiO_2 compound is added with 45-50 wt.% SiO_2, the CCT range declines to ∼700-750 K. However, based on the data, the generated light gradually shifted to cool, bright green color rather than warm white light. Henceforth, the white light of the prepared LED can have better lighting uniformity when the SLA: Yb/Er@SiO_2 compound is used with high SiO_2 amounts around 45-50 wt.%.

The presence of SLA: Yb/Er@SiO_2 can help induce the transmission power and luminous strength of LED light, as shown by Figure 4. Figure 4(a) depicts the LED light's transmitting intensity as a function of SLA: Yb/Er@SiO_2 addition. The data indicate that the presence of SLA: Yb/Er@SiO_2 with high SiO_2 doping amounts induced the transmission performance in the blue and green regions with the peaks at 450 and 545 nm, respectively. The red emission region showed no peak, implying that the red emission appearing in the phosphor luminescence was insufficient to cover the LED-light red spectral region when the YAG:Ce^{3+} appeared in the phosphor compound. Such two eminent peaks in the blue and green regions can be attributed to the improved forward scattering and conversion of the blue light from the blue chip with the addition of SLA: Yb/Er@SiO_2. The higher amounts of SiO_2 in the compound probably enhance the scattering performance of the blue light, inducing the absorption efficiency of the

green SLA: Yb^{3+}/Er^{3+} phosphor. Consequently, more green light is generated and propagated to combine with the transmitted blue and yellow light to form white light. Moreover, the high intensity of the green and blue emissions is beneficial to the white LED package's luminosity. To verify this, the lumen output of the prepared white LED package as a function of increasing SiO_2 content in the SLA: Yb/Er@SiO_2 compound is demonstrated in Figure 4(b). The higher the concentration of SiO_2 content, the better the lumen output. Hence, phosphor could be a promising upconversion-green-emission material for LED devices requiring enhanced luminosity (Fjodorow et al., 2022; Liu et al., 2022; Zhang et al., 2022).

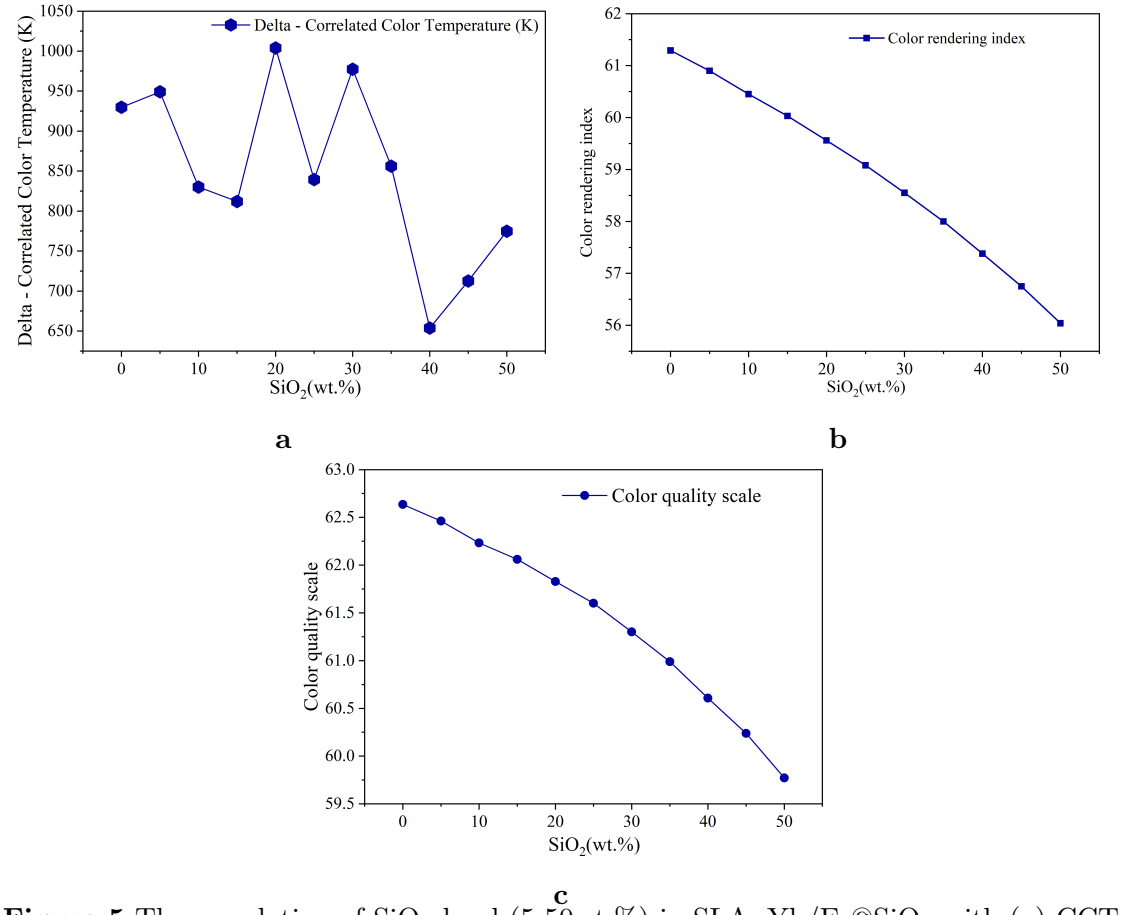

Figure 5 The correlation of SiO_2 level (5-50wt.%) in SLA: Yb/Er@SiO_2 with (a) CCT deviation values, (b) Color rendering index, and (c) Color quality scale of LED light

The performance of color rendition is demonstrated via CCT deviation, color rendering index, and color quality scale. The color uniformity of the LED light can be evaluated using the CCT deviation. A lower CCT deviation results in higher color uniformity. Figure 5(a) demonstrates the LED-light CCT deviation (D-CCT) values when doping SLA: Yb/Er@SiO_2 phosphor compound. The significant fluctuation in D-CCT values in the presence of increasing SiO_2 concentration in the compound. When the compound comprised SiO_2 amounts of 5, 20, and 30 wt.%, the D-CCT of the LED using SLA: Yb/Er@SiO_2 was higher than that of the one without the compound, with 20 wt.% resulting in the highest D-CCT. This could be ascribed to the inconsistency in the emission color distribution caused by the scattering inducement. The scattering events could cause a change in the proportion of light color that participates in forming white light, thus creating a considerable fluctuation. Nevertheless, with other concentrations of SiO_2, the D-CCT values were lower than the reference value (at 0 wt.% SiO_2), especially bottoming out at ~645 K with 40 wt.% SiO_2 in SLA: Yb/Er@SiO_2. Moreover, with high concentrations of SiO_2 of ~40-50 wt.%, the D-CCT declines to be half or more than half of the reference D-CCT value. This means that the addition of green phosphor SLA: Yb/Er@SiO_2 could contribute to obtaining high chromatic uniformity (Anh et al., 2025a; Li et al., 2022).

However, the color rendering performance of the LED light did not favour the SLA: Yb/Er@SiO_2 presence, especially when the SiO_2 content increased. This is due to the surplus green emission energy but insufficient orange-red emission. This was demonstrated through the declining values of the color rendering index (Figure 5b) and color quality scale (Figure 5c). This time, the LED light showed a bright green emission, which is nearly monochromatic, which is more suitable for high-luminescence devices (Le et al., 2026; Anh et al., 2025b).

4. Conclusions

In this study, the SLA: Yb/Er@SiO_2 phosphor compound with strong green emission through an upconversion mechanism was proposed for use in high-luminescence LED light. The most suitable concentrations of ion dopants in the $SrLaAlO_4$ host were approximately 2 mol% of Er^{3+} and 4 mol% of Yb^{3+}. The emission spectra of SLA: Yb^{3+}/Er^{3+} show notable emission centers in both green (531-553 nm) and red (655-675 nm) regions when excited with a 980-nm infrared laser. For the optical performance of the fabricated LED light with SLA: Yb/Er@SiO_2 and YAG:Ce^{3+} compound and blue LED chip, the luminescence and transmission power were enhanced with increasing SiO_2 concentration in SLA: Yb/Er@SiO_2 green phosphor compound. The SLA: Yb/Er@SiO_2 presence also contributed to the maintenance of CCT stability by decreasing the YAG:Ce^{3+} concentration in accordance to its SiO_2 increasing concentration. In addition, the color uniformity of the LED light could be enhanced by increasing the SiO_2 content. The green-phosphor compound SLA: Yb/Er@SiO_2 can be a potential material upconversion material for solid-state lighting advancement. However, future studies on improving the color rendering performance of this SLA: Yb/Er@SiO_2 compound or single SLA: Yb^{3+}/Er^{3+} composition need to be carried out to extend the application of this green phosphor for superior LED devices.

Acknowledgements

The author wishes to express their gratitude to the Posts and Telecommunications Institute of Technology, Vietnam, for financial support for this research.

Author Contributions

Phan Xuan Le: Conceptualization, Methodology, Software, Validation, Formal analysis, Investigation, Data Curation, Writing, Review, Editing, Project administration.

Nguyen Thi Phuong Loan: Methodology, Investigation, Data Curation, Writing, Review, Editing, Visualization, Supervision, Funding acquisition.

Conflict of Interest

Authors state no conflict of interest.

References

Anh, N. D. Q., Ho, S. D., Man, P. T. M., Duy, T. K., & Loan, N. T. P. (2025a). Enhancing LED chromaticity and luminosity using SiO_2 particles with varying diameters. *Journal of Advanced Engineering and Computation*, *9*(1), 21–28. https://doi.org/10.55579/jaec.202591.476

Anh, N. D. Q., & Lee, H. Y. (2024). Incorporation of TiO_2 in vanadate red phosphor compounds for white light-emitting diodes. *Optoelectronics and Advanced Materials-Rapid Communications*, *18*, 480–484.

Anh, N. D. Q., Loan, N. T. P., Van De, P., & Lee, H. (2025b). Potassium bromide scattering simulation for enhancing phosphor-converted white light-emitting diode performance. *Optoelectronics and Advanced Materials-Rapid Communications*, *19*(7–8), 378–383.

Cao, X., Lian, Y., Liu, Z., Zhou, H., Wang, B., Zhang, W., & Huang, B. (2022). Hyperspectral image super-resolution via a multi-stage framework without spatial degradation. *Optics Letters*, *47*(19), 5184–5187. https://doi.org/10.1364/OL.473020

Chen, M. J., Loan, N. T. P., Tho, L. V., Bui, T., Le, P. X., Anh, N. D. Q., Liao, H. Y., Chang, J. C., & Lee, H. Y. (2020). Effects of $Ba_2Li_2Si_2O_7$:Sn^{2+}, Mn^{2+} and $CaMgSi_2O_6$:Eu^{2+}, Mn^{2+} particles on the optical properties of remote phosphor LED. *Materials Science-Poland*, *38*(1). https://doi.org/10.2478/msp-2020-0002

Chou, L. T., Wu, S. H., Hung, H. H., Lin, W. Z., Chen, Z. P., Ivanov, A. A., & Chia, S. H. (2022). Compact multicolor two-photon fluorescence microscopy enabled by tailorable continuum generation. *Optics Express*, *30*(22), 40315–40327. https://doi.org/10.1364/OE.470602

Cong, P. H., & Anh, N. D. Q. (2025). Enhancing chromatic performance of WLEDs using $Sr_8ZnSc(PO_4)_7$:Eu^{2+}@SiO_2. *Science and Technology Indonesia*, *10*, 467–472. https://doi.org/10.26554/sti.2025.10.2.467-472

Cong, P. H., Loan, N. T. P., Anh, N. D. Q., & Lee, H. Y. (2025). Influence of potassium bromide phosphor on optical properties of white light-emitting diodes. *International Journal of Advances in Applied Sciences*, *14*(4), 1359–1366. https://doi.org/10.11591/ijaas.v14.i4.pp1359-1366

Deng, W., Huang, D., Yang, F., Peng, J., You, W., & Ye, X. (2024). Design of high-efficiency broadband cyan phosphors for low-blue full-spectrum LED lighting. *Journal of Alloys and Compounds*, *1008*, 176579. https://doi.org/10.1016/j.jallcom.2024.176579

Fjodorow, P., Frolov, M. P., Korostelin, Y. V., Kozlovsky, V. I., Schulz, C., Leonov, S. O., Skasyrsky, Y. K., & Yuryshev, N. N. (2022). Intracavity absorption spectroscopy using a Cr:CdSe laser. *Optics Express*, *30*(22), 40347–40356. https://doi.org/10.1364/OE.471851

Gaudfrin, K., Lopez, J., Gemini, L., Delaigue, M., Hönninger, C., Kling, R., & Duchateau, G. (2022). Fused silica ablation by double ultrashort laser pulses with dual wavelengths and variable delays. *Optics Express*, *30*(22), 40120–40135. https://doi.org/10.1364/OE.461502

Hanh, N. T. M., Loan, N. T. P., & Anh, N. D. Q. (2025). Application of YF_3:Er^{3+},Yb^{3+} and $MgSr_3Si_2O_8$:Eu^{2+},Mn^{2+} layers in remote phosphor LED. *Telkomnika*. https://doi.org/10.12928/telkomnika.v18i6.13827

Kumari, A., Nayak, P., Patra, B., Venkatasubbaiah, K., & Das, R. (2022). Third-order nonlinear optical manifestations in intramolecular proton transfer fluorophores. *Journal of the Optical Society of America B*, *39*(10), 2857. https://doi.org/10.1364/JOSAB.467995

Le, P. X., Ho, S. D., Anh, N. D. Q., & Lee, H. Y. (2021). Triple-layer remote phosphor structure for enhancing color quality and luminous efficiency of WLEDs. *Materials Science-Poland*, *39*(4), 458–466. https://doi.org/10.2478/msp-2021-0037

Le, P. X., Loan, N. T. P., & Anh, N. D. Q. (2026). Optical assessment of TiO_2 in phosphor-converted WLED devices. *Science and Technology Indonesia*, *11*(1), 345–355. https://doi.org/10.26554/sti.2026.11.1.345-355

Le, P. X., Loan, N. T. P., Anh, N. D. Q., & Lee, H. Y. (2025). Thermally stable sol-gel yttrium aluminum garnet cerium phosphors for white light-emitting diodes. *International Journal of Advances in Applied Sciences*, *14*(4), 1367–1374. https://doi.org/10.11591/ijaas.v14.i4.pp1367-1374

Le, P. X., Trang, T. T., Anh, N. D. Q., Lee, H. Y., & Tho, L. V. (2022). Comparison of $CaCO_3$ and TiO_2 scattering particles for improving color uniformity and luminous flux of WLEDs. *Materials Science-Poland*, *40*(1), 1–8. https://doi.org/10.2478/msp-2022-0008

Li, Y., Shi, X., Yang, L., Pu, C., Tan, Q., Yang, Z., & Huang, H. (2022). MC-GAT: Multi-layer collaborative generative adversarial transformer for hyperspectral image classification. *Biomedical Optics Express*, *13*(11), 5794–5812. https://doi.org/10.1364/BOE.472106

Liang, H., Yang, G., Bai, S., Li, C., Li, X., Wang, Y., Huang, J., Ji, J., & Zhu, Y. (2022). Efficient and tunable photoluminescence in terbium-doped Cs_2NaYCl_6 double perovskites. *Optics Letters*, *47*(19), 5176–5179. https://doi.org/10.1364/OL.472170

Lin, S., Sun, P., Gao, H., & Ju, Z. (2022). Nighttime image dehazing based on haze optical modeling. *Journal of the Optical Society of America A*, *39*(10), 1893–1902. https://doi.org/10.1364/JOSAA.463033

Liu, C., Zou, Z., Miao, Y., & Qiu, J. (2022). Light field quality assessment based on aggregation learning of multiple visual features. *Optics Express*, *30*(21), 38298–38318. https://doi.org/10.1364/OE.467754

Loan, N. T. P., & Anh, N. D. Q. (2021). Enhancing optical performance of dual-layer remote phosphor structures using $LaAsO_4$:Eu^{3+} and Y_2O_3:Ho^{3+} [Available online].

Loan, N. T. P., Anh, N. D. Q., Trang, N. C., & Lee, H. Y. (2022). Improved color uniformity and luminous intensity using three-layer remote phosphor structures for LEDs. *Materials Science-Poland*, *40*(1), 60–67. https://doi.org/10.2478/msp-2022-0010

Luo, G. F., Loan, N. T. P., Tho, L. V., That, P. T., Anh, N. D. Q., Chen, M. J., Liao, H. Y., & Lee, H. Y. (2020). Enhancing lighting performance of WLEDs using dual-layer remote phosphor configurations. *Materials Science-Poland*. https://doi.org/10.2478/msp-2020-0044

Lv, C., Li, C., Xiao, K., & Gao, C. (2022). Spectral image compression and reproduction based on colorimetric value mapping. *Optics Express*, *30*(22), 40144–40160. https://doi.org/10.1364/OE.468166

Ma, Y., Wang, Z., Pang, T., Lin, S., Wu, L., Xi, G., Zeng, L., Lu, L., Fu, Y., Tian, Y., Li, X., Wang, G., Chen, S., & Chen, D. (2024). Cyan-green-emitting garnet-structured $Lu_3ScAl_2ScAl_3O_{12}$:Ce^{3+} phosphor ceramics for high-color-quality laser-driven lighting. *Ceramics International*. https://doi.org/10.1016/j.ceramint.2024.03.216

My, L. T. T., Thai, N. L., Bui, T. M., Lee, H. Y., & Anh, N. D. Q. (2023). Phosphor conversion for WLEDs: YBO_3:Ce^{3+},Tb^{3+} and its effects on luminous intensity and chromatic properties. *Materials Science-Poland*, *40*(4), 105–113. https://doi.org/10.2478/msp-2022-0050

Nguyen, T. P. L., Nguyen, D. Q. A., Phan, T. M. M., & Lee, H. Y. (2025). Assessment of thermal degradation in yttrium aluminum garnet phosphor precursors. *Science and Technology Indonesia*, *10*(4), 1209–1214. https://doi.org/10.26554/sti.2025.10.4.1209-1214

Nguyen, V. D., & Nguyen, D. Q. A. (2025). $Ba_3GdNa(PO_4)_3F$:Eu^{2+} phosphor with blue-red emission characteristics for white LEDs. *International Journal of Electrical and Computer Engineering*, *38*(3), 1564–1571. https://doi.org/10.11591/ijeecs.v38.i3.pp1564-1571

Sun, X., Liang, Y., Zheng, J., Zhao, C., Fang, Z., Tian, T., Liang, X., Huan, W., & Xiang, W. (2024). High-brightness and high-stability Ce:YAG phosphor-in-glass for advanced laser lighting. *Ceramics International*, *50*, 48909–48917. https://doi.org/10.1016/j.ceramint.2024.09.341

That, P. T., Bui, T. M., Loan, N. T. P., Le, P. X., Anh, N. D. Q., & Tho, L. V. (2020a). Dual-layer remote phosphor structure for enhancing color quality and luminous flux of WLEDs. *International Journal of Electrical and Computer Engineering*, *10*(4), 4015–4022. https://doi.org/10.11591/ijece.v10i4.pp4015-4022

That, P. T., Loan, N. T. P., Tho, L. V., Anh, N. D. Q., Liao, H. Y., Luo, G. F., & Lee, H. Y. (2020b). Enhancing color quality of WLEDs using dual-layer remote phosphor geometry. *Materials Science-Poland*. https://doi.org/10.2478/msp-2020-0070

Thi, M. H. N., Bui, T. M., & Anh, N. D. Q. (2021). Influence of SiO_2 nanoparticles on photoluminescence enhancement of YAG:Ce phosphor. *International Journal of Electrical and Computer Engineering*, *11*(6), 4833–4839. https://doi.org/10.11591/ijece.v11i6.pp4833-4839

Thi, M. H. N., That, P. T., & Anh, N. D. Q. (2020). Eu^{2+}-activated strontium-barium silicate phosphors for improving luminous efficacy and color uniformity of LEDs. *Materials Science-Poland*. https://doi.org/10.2478/msp-2020-0069

Thuy, M. L. T., Le, T. N., Minh, B. T., Lee, H. Y., & Anh, N. D. Q. (2022). Phosphor conversion for WLEDs: YBO_3:Ce^{3+},Tb^{3+} and its impact on luminous and chromatic properties. *Materials Science-Poland*, *40*(4), 105–113.

Trang, L. T., & Anh, N. D. Q. (2025). Influence of SiO_2 particles on optical properties of white light-emitting diodes via simulation. *Indonesian Journal of Electrical Engineering and Computer Science*, *38*(3), 1572–1579. https://doi.org/10.11591/ijeecs.v38.i3.pp1572-1579

Trang, L. T., Loan, N. T. P., Cong, P. H., Anh, N. D. Q., & Lee, H. Y. (2025). Optical simulation of phosphor-converted WLEDs using barium sulfate for performance enhancement. *International Journal of Advances in Applied Sciences*, *14*(4), 1384–1392. https://doi.org/10.11591/ijaas.v14.i4.pp1384-1392

Tung, H. T., Anh, N. D. Q., & Lee, H. Y. (2024a). Impact of phosphor particle size and concentration on luminous efficiency of white light-emitting diodes. *Optoelectronics and Advanced Materials-Rapid Communications*, *18*(1–2), 58–65.

Tung, H. T., Loan, N. T. P., & Anh, N. D. Q. (2024b). Enhancing chromatic uniformity and luminous flux of WLEDs using dual-layer phosphor configurations. In *Recent advances in electrical engineering and related sciences* (pp. 167–174). Springer. https://doi.org/10.1007/978-981-99-8703-0_14

Tung, H. T., Minh, B. T., Thai, N. L., Lee, H. Y., & Anh, N. D. Q. (2024c). ZnO particles as scattering centers for improving color quality and luminous efficiency of WLEDs.

Wang, Y., Cheng, Z., Ye, J., Zhu, D., Hu, C., Zhou, Z., & Li, T. (2025). Effect of Ga^{3+} content on luminous properties of Ce^{3+}-doped $Lu_2YGaxAl_{5-x}O_{12}$ phosphor ceramics. *Journal of Luminescence*, *280*, 121115. https://doi.org/10.1016/j.jlumin.2025.121115

Zhan, B., Wang, Y., & Seto, T. (2024). Broadband yellow-emitting oxynitride phosphor $Sr_2Si_7Al_3ON_{13}$:Ce^{3+},Eu^{2+} for high-color-rendering LEDs. *Inorganic Chemistry*, *63*(16), 7334–7342. https://doi.org/10.1021/acs.inorgchem.4c00234

Zhang, H., Tu, S., Li, L., Chen, X., Zhao, Y., Wu, M., Zhang, X., Zhang, S., & Chen, L. (2022). Large-scale transparency-adjustable mini-LED display using electrochromic shutter technology. *Optics Express*, *30*(22), 39904–39910. https://doi.org/10.1364/OE.469659